

# High gain hot-carrier WSe<sub>2</sub> phototransistor with gate-tunable responsivity

Yuxuan Jin<sup>1,2, a</sup>, Zefeng Chen<sup>1,2, b</sup>

1. School of Optoelectronic Science and Engineering & Collaborative Innovation Center of Suzhou Nano Science and Technology, Soochow University, Suzhou 215006, China;

2. Key Lab of Advanced Optical Manufacturing Technologies of Jiangsu Province & Key Lab of Modern Optical Technologies of Education Ministry of China, Soochow University, Suzhou 215006, China;

<sup>a</sup>yxjin1106@stu.suda.edu.cn, <sup>b</sup>zfchen86@suda.edu.cn

**Abstract.** Hot-carrier injection at semiconductor/metal interface shows great potentials in infrared photodetection. However, the photoresponsivity of hot-carrier photodetector with diode mode is still limited in the scale of 1 mA/W due to the low injection efficiency of hot carriers and the lack of gain. Here, we demonstrate a high gain hot-carrier WSe<sub>2</sub> phototransistor with gate-tunable responsivity. In this device, plasmonic resonances is used to enhance the light absorption of gold nanodisk, which provide hot holes. The hot holes are trapped into WSe<sub>2</sub> and recycled in WSe<sub>2</sub> channel in lateral direction, which introduce high gain for photodetection. Experiment shows that the photoresponsivity of the device can be over 0.23 A/W with a gain of 270 at the wavelength of 1310 nm. More interestingly, the responsivity of the device can be tuned by gate, which can be used to encode synaptic weights of the sensor pixel.

**Keywords:** Infrared photodetector, plasmonic resonance, hot carrier, 2D materials.

## 1. Introduction

Photodetection of infrared light attracts great attention due to its important applications in optical communication, biological imaging, remote control, et al [1–3]. Most of infrared detectors are based on narrow-bandgap semiconductor such as In<sub>x</sub>Ga<sub>1-x</sub>As, and HgTe [4–5]. However, the fabrication of these semiconductors is usually complicated (e.g., based on molecular beam epitaxy) and environmentally unfriendly (i.e., contains arsenic and mercury). Besides, low temperature is generally required during the operation of these detectors.

Beyond photo-induced carriers in semiconductor, metal also can provide so-call hot carriers for photodetection, which have been demonstrated in recent ten years [6-9]. Through introducing plasmonic resonance to enhance the light absorption, infrared photodiode based on hot-carrier effect has been realized in many semiconductor/metal junctions (e.g., Si/Ti, TiO<sub>2</sub>/Ag, et al.). However, due to the low injection rate of hot carriers, the photoresponsivity of hot-carrier photodiode is still lower than conventional infrared photodetector based on narrow-bandgap semiconductor [10–14]. A promising way to improve the photoresponsivity is to introduce the gain into the device.

In this work, we propose an infrared hot-carrier photodetector with high gain by stacking a 2D plasmonic gold nanodisk array on multilayer WSe<sub>2</sub> transistor. The hot holes are generated in the array of gold nanodisks with plasmonic resonance and trapped into WSe<sub>2</sub> channel working as the excess carriers in WSe<sub>2</sub>. Different from the hot-carrier photodiode, the hot holes are drifted in the WSe<sub>2</sub> channel by the lateral electrical field between source/drain to form photocurrent, which thus can be recycled in the channel. Experimental results show that this hot-carrier phototransistor exhibits a high photoresponsivity up to 0.23 A/W with a gain over 270 at the wavelength of 1310 nm, which is in the wavelength region far away from the absorption band of WSe<sub>2</sub>. More interestingly, the hot-carrier photodetector exhibits a tunable photoresponsivity by electrical gating, which is resulted from the gate-depended effective FET mobility of WSe<sub>2</sub> transistor.

## 2. Results and discussion

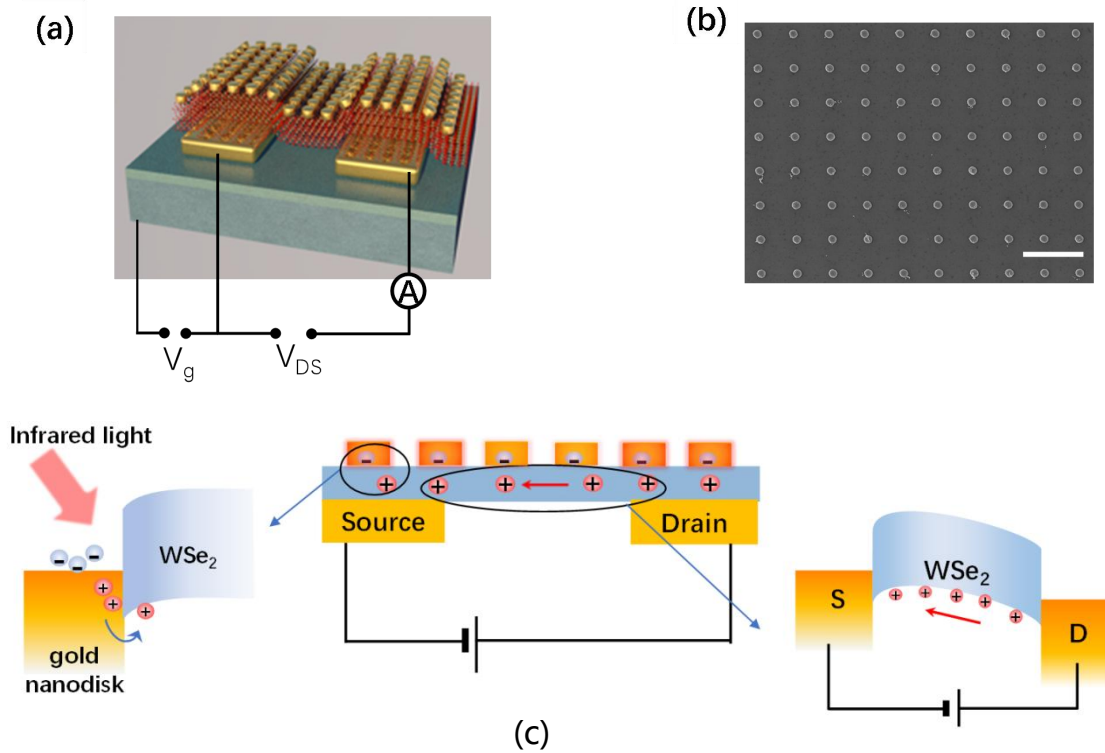


Figure 1 (a) Schematic of the device, where a top electrode contact  $\text{WSe}_2$  transistor is covered by gold nanodisk array. (b) SEM image of gold nanodisks on  $\text{WSe}_2$ . The scale bar is  $1 \mu\text{m}$ . (c) Schematic diagram of the hot-carrier  $\text{WSe}_2$  phototransistor with gain. Both two electrodes are load on  $\text{WSe}_2$ . Hot holes are trapped from gold nanodisks into  $\text{WSe}_2$  (left); The injected hot holes are driven in by lateral electrical field in  $\text{WSe}_2$  channel (right) and will be recycled within the lifetime.

The schematic of  $\text{WSe}_2$  hot-carrier phototransistor is shown in Figure 1(a), composed of gold electrodes (source/drain), plasmonic crystal (Au nanodisk array), dielectric layer ( $300 \text{ nm SiO}_2$ ) and bottom gate electrode ( $\text{p}^+\text{-Si}$ ). The  $\text{WSe}_2$  with thickness of  $40 \text{ nm}$  was exfoliated by mechanism exfoliation method and then dry-transferred to the prepared electrodes, forming a top contact field effect transistor (FET) [15–16]. Gold nanodisk array with diameter of  $160 \text{ nm}$  and period of  $700 \text{ nm}$  is fabricated on another silicon wafer by standard electronic photolithography and then transferred to the  $\text{WSe}_2$  FETs. The SEM images of gold nanodisk array on  $\text{WSe}_2$  FETs are shown in Figure 1(b). In this device, the gold electrodes act not only as source/drain, but also as bottom mirror for forming a metal-insulator-metal (MIM) plasmonic structure [17-18]. The plasmonic effect can be divided into two parts. One is localized plasmonic effect of individual gold nanodisk in the FET channel. The other is the MIM plasmonic resonance on the source and drain electrodes, where the multilayer  $\text{WSe}_2$  acts as cavity layer. Under SWIR light illumination, the light with wavelength matching will be trapped by the plasmonic effect of gold nanodisks. This light trapping will enhance the light absorption of gold, generating hot carriers in gold nanodisks. The hot carriers will then cross the Schottky barrier of  $\text{WSe}_2/\text{Au}$  junction and be trapped into the  $\text{WSe}_2$ , leading to the net increase of carrier concentration, as shown in the left of Figure 1(c). Under the bias of source/drain, the injection carriers in  $\text{WSe}_2$  forms photocurrent, as shown in the right of Figure 1(c). Obviously, the device structure is different from the hot-carrier photodiode, in which electrodes are loaded on metal plasmonic nanostructure (e.g., grating) and semiconductor. In photodiodes, the injected hot holes (electrons) in semiconductor and the hot electrons (holes) will recombine through

external circuit. Therefore, the hot carriers can hardly be recycled. In our device, the gold nanodisks only contribute to hot-carrier generation in vertical direction but not for carrier transport. The WSe<sub>2</sub> in this device is used to provide a lateral transport channel for the injected carriers. Therefore, the recombination rate of hot carriers will be largely reduced. If the lifetime of hot carriers is longer than the transit time in the WSe<sub>2</sub> channel, high responsivity and gain will be achieved.

The transfer curve of hot-carrier WSe<sub>2</sub> phototransistor under the infrared light illumination with different incident power is shown in Figure 2(a). Here, the wavelength of incident light is 1310 nm, which is a typical communication wavelength in infrared region. The transfer curve exhibits on-state at negative gate voltage, which indicates WSe<sub>2</sub> transistor has p-type channel. As the increase of incident power, evidently photocurrent is observed in the on-state region and the transfer curves shifts to the direction of positive voltage. For example, when the incident power increases from 0 to 298 nW, the threshold voltage is shifted from around -20 to -15 V, which indicates the increase of hole concentration. However, in the off-state region (-5 to 20 V), almost no photocurrent is observed (Figure 2(b)), which means the electron concentration remains unchanged. These phenomenon agrees well with that only hot holes are injected into WSe<sub>2</sub>. For comparison, we measure the photoresponse of WSe<sub>2</sub> phototransistor under the incident light with wavelength of 760 nm, in which photon induced carriers are mainly from the interband transition of WSe<sub>2</sub>, as shown in Figure 2(c). In this case, the transfer curve is uplifted and the photoresponse arises in both the on-state region and off-state region. This is a typical response of phototransistor with photon induced carrier from interband transition. With light illumination, electrons in valence band are excited to conduction band and holes are generated in valence band, forming both excess electrons and holes. The excess electrons (holes) are reflected by the photocurrent in the off-state (on-state) region of the transfer curve. Obviously, the efficiency of photon induced carrier from band transition should be much higher than hot carriers injection, which results the much higher photoresponse for the incident light with wavelength of 760 nm light.

From the discussion above, we can conclude that the photoresponse of our device in the short wavelength infrared region is mainly attributed to the hot carriers injection from the gold disks. The photocurrent induced by hot-carrier injection can be described as  $I_{light} - I_{dark} = e\mu_p\Delta p U \frac{W}{L}$ , where  $e$ ,  $\mu_p$ ,  $\Delta p$  and  $U$  are the unit charge, the effective hole mobility of transistor, the injected hot concentration and the bias voltage between source and drain, and  $W/L$  is the ratio between the width and length of transistor.

The photoresponsivity of this device can be calculated by the function  $R = \frac{I_{light} - I_{dark}}{Power}$ , as shown in Figure 2(d). The photoresponsivity is 0.23 A/W under 1310 nm light at the gate voltage of -40 V, which is much higher than the reported responsivity of hot-carrier photodetector at this wavelength [14]. The gain can be calculated by the function:  $G = \frac{\Delta I/e}{\alpha(P_{in}/\hbar\nu)\chi} = \eta/(\alpha\chi)$ , where  $\alpha$  presents conversion efficiency of photons to hot carriers in metal and  $\chi$  is the injection efficiency of hot hole from gold to WSe<sub>2</sub>. According to previous reports about hot-carrier injection from metal to semiconductor,  $\alpha$  is around 10% ~ 99% and  $\chi$  is down to 0.01 ~ 1% [14]. Therefore, if  $\alpha = 100\%$ , the gain of our device is estimated to be 270. The high gain can be attributed to its unique working mechanism. In the our WSe<sub>2</sub> device, only hot holes are injected into the WSe<sub>2</sub> channel and become excess holes, leaving electrons in gold nanodisks. Therefore, when the hot holes are driven by the lateral electrical field in the WSe<sub>2</sub> channel, they cannot find excess electrons to recombine with during the transport in WSe<sub>2</sub> channel. Thus, the hot holes (or excess hole) in WSe<sub>2</sub> can be recycled for many times, which results the high gain and responsivity.

Figure 2(d) also shows that the photoresponsivity can be tuned by gate voltage. For example, When the incident power is 125 nW the photoresponsivity is up to 0.23 A/W at the gate voltage of -40 V, while it decreases 0.027 A/W at the gate voltage of -20 V. According to the above function, the photocurrent is proportional to the effective hole mobility of transistor, which is depended on the gate voltage of the transistor. In WSe<sub>2</sub> transistor, the drain current is not only determined by the

carrier density of WSe<sub>2</sub> channel, but also the p-type Schottky contact between electrode and WSe<sub>2</sub> [19,20]. When a negative V<sub>g</sub> is applied, the electrostatic doping decreases the Fermi level of WSe<sub>2</sub> and the width of the barrier will be narrowed, which enables more carriers to inject into the channel to switch on the transistor by directing tunneling. Thus, when a lower voltage is applied, the holes will be easier to transfer from source to drain, which corresponds to the higher effective hole mobility of transistor.

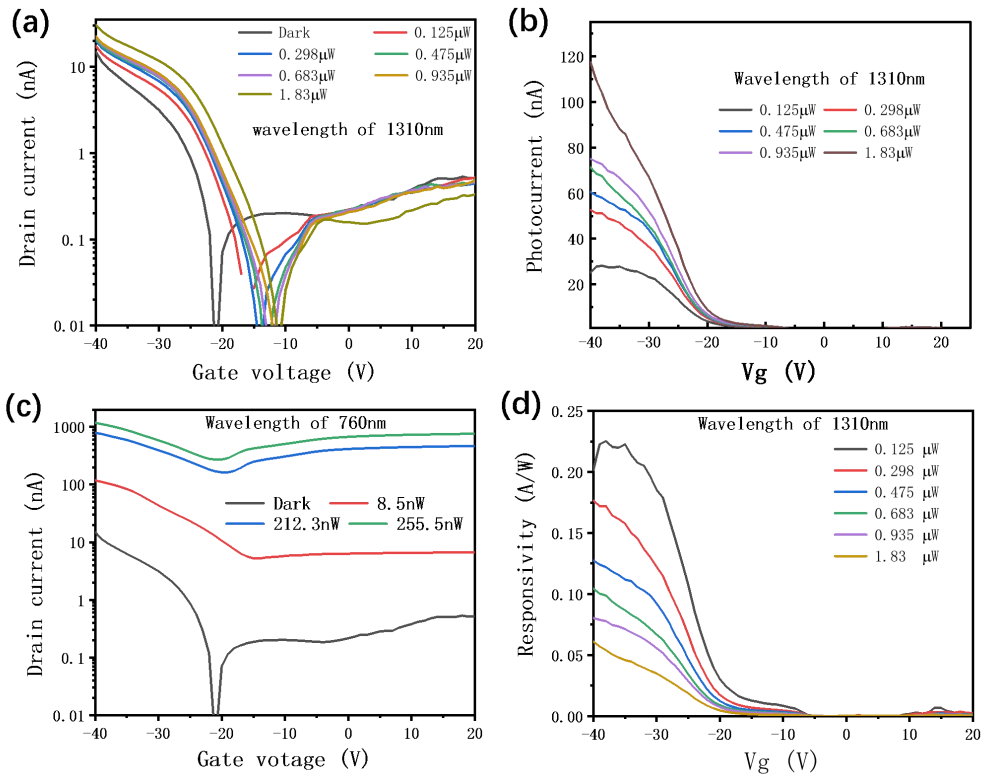


Figure 2 (a) Photoresponse of the WSe<sub>2</sub> hot carrier phototransistor under the illumination of 760 nm light with different incident power. (b) Photocurrent WSe<sub>2</sub> hot carrier phototransistor. (c) Photoresponse of the WSe<sub>2</sub> hot-carrier phototransistor under the illumination of 760 nm light with different incident power.

The transient photoresponse (response speed) is shown in Figure 3. When the laser is switched on, the rising time of transient photoresponse is about 60 ms. When the laser is switched off, the falling time is 150 ms, which is about much longer than rising time. Generally, the rising and falling times correspond to the carrier generation and recombination. Thus, the experimental transient photoresponse indicates the generation and recombination rate of photon induced carrier are not equal, which can be attributed to the hot-carrier injection model. When the laser is switched on, hot holes are excited in gold disk, then some of them are swept into WSe<sub>2</sub> by the built-in field of Schottky junction and become excess holes. As only hole is injected into WSe<sub>2</sub>, the excess holes cannot recombine with hot electrons in WSe<sub>2</sub> channel. Therefore, the recombination pathway for holes is diffusing back to gold, which takes a longer time.

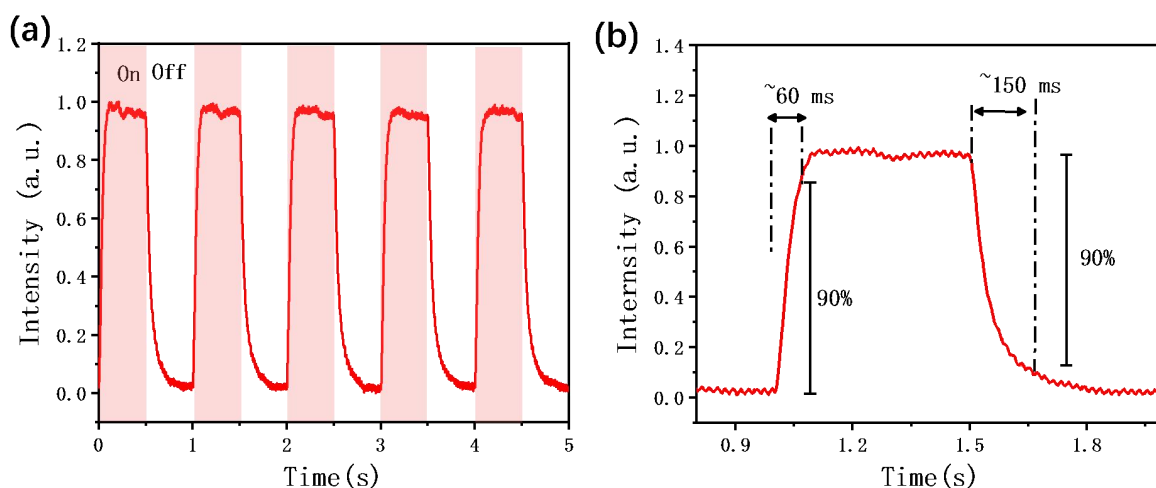


Figure 3 (a) Transient photoresponse of the device. (b) Zoom-in of (a).

### 3. Summary

We demonstrate an infrared hot-carrier photodetector composed of plasmonic gold nanodisk array on multilayer WSe<sub>2</sub> transistor. Different from the previous hot-carrier photodetector, this device exhibits high responsivity and high gain. The experimental results show that the hot holes are generated in the array of gold nanodisks with plasmonic resonance and injected into WSe<sub>2</sub> channel as excess carriers. The injected hole in WSe<sub>2</sub> is then driven by the lateral electrical field to form photocurrent with high gain. Interestingly, the hot-carrier WSe<sub>2</sub> photodetector exhibits tunable photoresponsivity by electrical gating, which is promising for encoding synaptic weights of the photosensor pixel in artificial neural network vision.

### References

- [1] Rogalski, A., Infrared detectors: status and trends. *Progress in quantum electronics* 2003, 27 (2–3), 59-210.
- [2] Tao, L.; Chen, Z.; Li, Z.; Wang, J.; Xu, X.; Xu, J. Enhancing light-matter interaction in 2D materials by optical micro/nano architectures for high-performance optoelectronic devices. *InfoMat* 2021, 3 (1), 36–60.
- [3] Long, M.; Wang, P.; Fang, H.; Hu, W., Progress, challenges, and opportunities for 2D material based photodetectors. *Advanced Functional Materials* 2019, 29 (19), 1803807.
- [4] Chaubet, M.; Mollier, J.; Sage, J.; Roizes, A.; Aubry, Y., Feasibility study of a new heterodyne technique based on HgCdTe varactor photodetectors for space-borne wind lidars. *Microwave and Optical Technology Letters* 1995, 8 (4), 179-184.
- [5] Myers, S.; Plis, E.; Kim, H. S.; Khoshakhlagh, A.; Gautam, N.; Lee, S. J.; Noh, S. K.; Krishna, S., Heterostructure engineering in Type II InAs/GaSb strained layer superlattices. *Physica status solidi c* 2010, 7 (10), 2506-2509.
- [6] Chalabi, H.; Schoen, D.; Brongersma, M. L., Hot-electron photodetection with a plasmonic nanostripe antenna. *Nano letters* 2014, 14 (3), 1374-1380.
- [7] García de Arquer, F. P.; Mihi, A.; Konstantatos, G., Large-area plasmonic-crystal-hot-electron-based photodetectors. *ACS photonics* 2015, 2 (7), 950-957.
- [8] Knight, M. W.; Sobhani, H.; Nordlander, P.; Halas, N. J., Photodetection with active optical antennas. *Science* 2011, 332 (6030), 702-704.

- [9] Sobhani, A.; Knight, M. W.; Wang, Y.; Zheng, B.; King, N. S.; Brown, L. V.; Fang, Z.; Nordlander, P.; Halas, N. J., Narrowband photodetection in the near-infrared with a plasmon-induced hot electron device. *Nature communications* 2013, 4 (1), 1643.
- [10] Li, W.; Valentine, J., Metamaterial perfect absorber based hot electron photodetection. *Nano letters* 2014, 14 (6), 3510-3514.
- [11] Lin, K.-T.; Chen, H.-L.; Lai, Y.-S.; Yu, C.-C., Silicon-based broadband antenna for high responsivity and polarization-insensitive photodetection at telecommunication wavelengths. *Nature communications* 2014, 5 (1), 3288.
- [12] Wen, L.; Chen, Y.; Liu, W.; Su, Q.; Grant, J.; Qi, Z.; Wang, Q.; Chen, Q., Enhanced photoelectric and photothermal responses on silicon platform by plasmonic absorber and omni-schottky junction. *Laser & Photonics Reviews* 2017, 11 (5), 1700059.
- [13] Zhang, C.; Wu, K.; Zhan, Y.; Giannini, V.; Li, X., Planar microcavity-integrated hot-electron photodetector. *Nanoscale* 2016, 8 (19), 10323-10329.
- [14] Zhang, C.; Luo, Y.; Maier, S. A.; Li, X., Recent progress and future opportunities for hot-carrier photodetectors: From ultraviolet to infrared bands. *Laser & Photonics Reviews* 2022, 16 (6), 2100714.
- [15] Das, S.; Appenzeller, J., WSe<sub>2</sub> field effect transistors with enhanced ambipolar characteristics. *Applied physics letters* 2013, 103 (10), 103501.
- [16] Yu, L.; Zubair, A.; Santos, E. J.; Zhang, X.; Lin, Y.; Zhang, Y.; Palacios, T., High-performance WSe<sub>2</sub> complementary metal oxide semiconductor technology and integrated circuits. *Nano letters* 2015, 15 (8), 4928-4934.
- [17] Liu, N.; Mesch, M.; Weiss, T.; Hentschel, M.; Giessen, H., Infrared perfect absorber and its application as plasmonic sensor. *Nano letters* 2010, 10 (7), 2342-2348.
- [18] Aydin, K.; Ferry, V. E.; Briggs, R. M.; Atwater, H. A., Broadband polarization-independent resonant light absorption using ultrathin plasmonic super absorbers. *Nature communications* 2011, 2 (1), 517.
- [19] Wang, Z.; Li, Q.; Chen, Y.; Cui, B.; Li, Y.; Besenbacher, F.; Dong, M., The ambipolar transport behavior of WSe<sub>2</sub> transistors and its analogue circuits. *NPG Asia Materials* 2018, 10 (8), 703-712.
- [20] Pradhan, N.; Rhodes, D.; Memaran, S.; Poumirol, J.; Smirnov, D.; Talapatra, S.; Feng, S.; Perea-Lopez, N.; Elias, A.; Terrones, M., Hall and field-effect mobilities in few layered p-WSe<sub>2</sub> field-effect transistors. *Scientific reports* 2015, 5 (1), 8979.